1-2009

Non-primitive rectangular cells for tight-binding electronic structure calculations

Timothy Boykin
University of Alabama - Huntsville

Neerav Kharche
Birck Nanotechnology Center and Purdue University, nkharche@purdue.edu

Gerhard Klimeck
Network for Computational Nanotechnology, Purdue University, gekco@purdue.edu

Physica E 41 (2009) 490–494

Contents lists available at ScienceDirect

Physica E

journal homepage: www.elsevier.com/locate/physe

Non-primitive rectangular cells for tight-binding electronic structure calculations

Timothy B. Boykin [a,*], Neerav Kharche [b], Gerhard Klimeck [b,1]

[a] Department of Electrical and Computer Engineering, The University of Alabama in Huntsville, Huntsville, Alabama 35899, USA
[b] Network for Computational Nanotechnology, School of Electrical and Computer Engineering, Purdue University, West Lafayette, Indiana 47907, USA

ARTICLE INFO

Article history:
Received 14 May 2008
Accepted 30 September 2008
Available online 5 November 2008

PACS:
7.15.−m
73.21.−b

Keywords:
Brillouin zone
Allowed wavevectors
Zone unfolding

ABSTRACT

Rectangular non-primitive unit cells are computationally convenient for use in nanodevice electronic structure and transport calculations. When these cells are used for calculations of structures with periodicity, the resulting bands are zone-folded and must be unfolded in order to identify important gaps and masses. Before the zone-unfolding method can be applied, one must first determine the allowed wavevectors for the specific non-primitive cell. Because most computationally convenient non-primitive cells do not have axes parallel to the primitive cell direct lattice vectors, finding the allowed wavevectors is generally a non-trivial task. (Solid state texts generally treat only the simplest case in which the non-primitive and primitive cell axes are all aligned.) Rectangular non-primitive cells with one axis aligned along a specific direction are especially useful for obtaining the approximate random-alloy bands for a bulk crystal, a critical verification step in any random-alloy nanostructure calculation. Here, we present an easily implemented method for determining a non-primitive rectangular cell for the FCC lattice with an axis aligned in a desired direction and the associated allowed primitive cell wavevectors. We illustrate its use by unfolding the bands of Ge.

1. Introduction

Technologically important semiconductor nanostructures, such as quantum wells, resonant-tunneling diodes, superlattices, and nanowires feature materials changes on a nanometer scale and are, therefore, readily modeled using the tight-binding method. These structures are most often fabricated from semiconductors such as Si, Ge, GaAs, and InAs, which adopt cubic symmetry in bulk. In the presence of regular strain, the symmetry is reduced, but rectangular geometry persists. Multi-band tight-binding modeling tools, such as NEMO3D [1] are very complicated, and the underlying mathematics and programming are greatly simplified if the calculation is based on a non-primitive rectangular unit cell. For modeling nonperiodic structures such as quantum dots, the use of a non-primitive cell poses no problems. In contrast, when structures with periodicity (such as bulk alloys, superlattices, or quantum wells) are modeled with a non-primitive cell, the resulting bands are zone-folded, so that identifying important gaps and effective masses becomes difficult.

Alloy nanostructures pose challenges beyond those present in nanostructures made of pure materials. Improving upon the virtual crystal approximation involves random-alloy supercell methods [2,3]. In these calculations an essential first step is about verifying the accuracy of the tight-binding random-alloy treatment of the bulk, which generally involves probing the calculated (approximate) bands along several relevant symmetry directions in order to compare the results to the known energy gaps and effective masses. When the supercell used is composed of many non-primitive rectangular cells, the zone-folding is especially severe. Due to the mathematics of zone unfolding [4] choosing non-primitive rectangular cells aligned along the desired direction yields the greatest density of small-cell wavevectors [2,4–6].

Determining the allowed small-cell wavevectors for tight-binding supercell calculations is sufficiently different from the special-*k*-points problem in Brillouin zone integration [7,8] and generally more difficult than the simple supercell problem treated in solid state texts [9–12] that these methods are not directly applicable. First, the supercells often do not have axes parallel to the primitive cell axes. Second, very often one has a supercell composed of non-primitive cells, with different numbers of non-primitive cells along the three non-primitive cell axes, so that the allowed small-cell wavevectors are sums of the supercell wavevectors and those for the non-primitive unit cell.

More pertinently, the different aims of Fourier quadrature and zone unfolding require different supercells. Fourier quadrature

* Corresponding author.
E-mail address: boykin@ece.uah.edu (T.B. Boykin).
[1] Also Jet Propulsion Laboratory, California Institute of Technology, Pasadena, CA 91109, USA.

1386-9477/$ - see front matter © 2008 Elsevier B.V. All rights reserved.
doi:10.1016/j.physe.2008.09.022

[7,8] is concerned with approximating the integral of a function over the *entire* Brillouin zone to a given accuracy, unlike zone unfolding which probes the bands along a given direction using a supercell composed of computationally convenient non-primitive cells. In zone unfolding, *all* allowed **k** must be retained and it is generally desirable to have a greater density of **k** in certain directions. In contrast, Fourier quadrature [7,8] *reduces* the number of **k** and specifies the smallest **R** for which the Fourier series fails to exactly integrate, implying a fairly uniform supercell. (The shortest supercell axis defines the smallest **R** for which exact integration fails). Specifically, neither of Refs. [7,8] treats the 6-FCC non-primitive cell here, and in fact the only FCC supercell considered in Ref. [7] is a supercell composed of the *same number* of 4-FCC non-primitive cells along each axis. Most of the supercells discussed in Refs. [7,8], thus are not of use in Brillouin zone unfolding for the FCC lattice. Most importantly, neither of Refs. [7,8] gives general formulas for constructing non-primitive cells with axes along a desired direction. The simple cubic cell discussed in Ref. [7] is, after all, not optimal for all applications. Thus a straightforward, easily implemented, method for finding these wavevectors in a rectangular non-primitive cell with one axis aligned in a desired direction is needed.

Here, we provide some simple formulas for choosing non-primitive rectangular cells in the face-centered cubic (FCC) lattice with one axis aligned along an arbitrary direction. These results are, therefore, directly applicable to tight-binding supercell calculations for diamond and zincblende semiconductors. Furthermore, the general approach detailed here can be adapted to finding non-primitive cells and allowed wavevectors for nanostructures such as quantum wells, superlattices, and nanowires [3,6]. In Section 2, we begin with some general results for non-primitive cells and allowed small-cell wavevectors, then specialize to formulas appropriate for the FCC lattice. In Section 3, we use these results to find the allowed wavevectors for three different non-primitive rectangular cells. As an example, we unfold the bands of Ge calculated with the 6-FCC cell. Section 4 presents our conclusions.

2. Method

2.1. General

A non-primitive cell is defined by direct lattice vectors $\mathbf{A}_i$, not necessarily orthogonal, which are decomposed in terms of the primitive cell direct lattice vectors $\mathbf{a}_j$ as

$$\mathbf{A}_i = \sum_{j=1}^{3} m_{i,j}\mathbf{a}_j, \quad i = 1,2,3; m_{i,j} \in \mathbb{Z}. \tag{1}$$

(For an alloy approximate bandstructure calculation all of the primitive cells still have the same dimensions but they are not all identical due to the different species or displacement of atoms within the cell and are more properly called small cells). The integers $m_{i,j}$ may be positive or negative and are conveniently arranged as a matrix $\underline{\mathbf{M}}$:

$$[\underline{\mathbf{M}}]_{i,j} = m_{i,j}. \tag{2}$$

We remark that the supercell treatment found in most solid state texts concerns only the very simplest case, that of a diagonal matrix with positive elements: $m_{i,j} = m_{i,i}\delta_{i,j}, m_{i,i} > 0$. A little algebra shows that

$$\mathbf{A}_1 \bullet (\mathbf{A}_2 \times \mathbf{A}_3) = \det(\underline{\mathbf{M}})[\mathbf{a}_1 \bullet (\mathbf{a}_2 \times \mathbf{a}_3)] \tag{3}$$

which implies that the integer $|\det(\underline{\mathbf{M}})|$ gives the number of primitive cells in the non-primitive cell, since the non-primitive cell volume is $|\mathbf{A}_1 \cdot (\mathbf{A}_2 \times \mathbf{A}_3)|$ while that of the small cell is $|\mathbf{a}_1 \cdot (\mathbf{a}_2 \times \mathbf{a}_3)|$.

The reciprocal lattice vectors of the non-primitive cell $\mathbf{B}_i$ are related to those of the small cell $\mathbf{b}_j$ in a like manner. In terms of the direct lattice vectors, the reciprocal lattice vectors are given by the usual relations [9]:

$$\boldsymbol{\beta}_1 = 2\pi \frac{\boldsymbol{\alpha}_2 \times \boldsymbol{\alpha}_3}{\boldsymbol{\alpha}_1 \bullet (\boldsymbol{\alpha}_2 \times \boldsymbol{\alpha}_3)}, \quad \boldsymbol{\beta}_2 = 2\pi \frac{\boldsymbol{\alpha}_3 \times \boldsymbol{\alpha}_1}{\boldsymbol{\alpha}_1 \bullet (\boldsymbol{\alpha}_2 \times \boldsymbol{\alpha}_3)}, \quad \boldsymbol{\beta}_3 = 2\pi \frac{\boldsymbol{\alpha}_1 \times \boldsymbol{\alpha}_2}{\boldsymbol{\alpha}_1 \bullet (\boldsymbol{\alpha}_2 \times \boldsymbol{\alpha}_3)}, \tag{4}$$

where $(\boldsymbol{\alpha},\boldsymbol{\beta}) = \{(\mathbf{a},\mathbf{b}),(\mathbf{A},\mathbf{B})\}$ as appropriate. Because the $m_{i,j}$ are integers Eqs. (1) and (3) imply that the non-primitive cell and small-cell reciprocal lattice vectors are related by rationals $w_{i,j}$:

$$\mathbf{B}_i = \sum_{j=1}^{3} w_{i,j}\mathbf{b}_j, \quad i = 1,2,3; \quad w_{i,j} \in \mathbb{Q}. \tag{5}$$

As before, the $w_{i,j}$ are conveniently arranged as elements of a matrix $\underline{\mathbf{W}}$:

$$[\underline{\mathbf{W}}]_{i,j} = w_{i,j}. \tag{6}$$

The matrices $\underline{\mathbf{M}}$ and $\underline{\mathbf{W}}$ are in fact related by $\underline{\mathbf{W}}^T = \underline{\mathbf{M}}^{-1}$, as can be seen from a simple calculation

$$\begin{aligned}\delta_{i,j} &= \frac{1}{2\pi}\mathbf{A}_i \bullet \mathbf{B}_j = \frac{1}{2\pi}\sum_{l=1}^{3}\sum_{n=1}^{3} m_{i,l}w_{j,n}(\mathbf{a}_l \bullet \mathbf{b}_n) \\ &= \frac{1}{2\pi}\sum_{l=1}^{3}\sum_{n=1}^{3} m_{i,l}w_{j,n}(2\pi\delta_{l,n})\end{aligned} \tag{7}$$

$$\delta_{i,j} = \sum_{l=1}^{3} m_{i,l}w_{j,l} = \sum_{l=1}^{3}[\underline{\mathbf{M}}]_{i,l}[\underline{\mathbf{W}}^T]_{l,j} = [\underline{\mathbf{M}}\,\underline{\mathbf{W}}^T]_{i,j}. \tag{8}$$

Eqs. (8) and (5) thus lead to the useful relation

$$\mathbf{b}_i = \sum_{l=1}^{3} m_{l,i}\mathbf{B}_l, \tag{9}$$

showing that, as required, the volume of the primitive cell Brillouin zone is $|\det(\underline{\mathbf{M}})|$ times as large as the supercell Brillouin zone.

Because the primitive cell Brillouin zone is $|\det(\underline{\mathbf{M}})|$ times larger than that of the non-primitive cell, there are $|\det(\underline{\mathbf{M}})|$ allowed small-cell wavevectors, onto which the non-primitive cell eigenstates are unfolded. These allowed small-cell wavevectors, **q**, are found by requiring [5]

$$\exp(i\mathbf{q} \bullet \mathbf{A}_j) = 1 \Rightarrow \mathbf{q} \bullet \mathbf{A}_j = 2p\pi, \quad p \in \mathbb{Z}, \quad j = 1,2,3. \tag{10}$$

Eq. (10) immediately implies that the allowed small-cell wavevectors are non-primitive cell reciprocal lattice vectors

$$\mathbf{q}_i = \sum_{j=1}^{3} n_{i,j}\mathbf{B}_j, \quad i = 0,1,\ldots,|\det(\underline{\mathbf{M}})| - 1; \quad n_{i,j} \in \mathbb{Z}, \tag{11}$$

with the restriction that none of the $\mathbf{q}_i$ are related by a primitive cell reciprocal lattice vector

$$\mathbf{q}_l - \mathbf{q}_m \neq \sum_{j=1}^{3} p_j\mathbf{b}_j, \quad p_j \in \mathbb{Z}. \tag{12}$$

These results are not specific to a particular primitive or non-primitive cell, or even to rectangular cells. To proceed further, the primitive and non-primitive cells must be specified. The most broadly applicable results can be obtained by considering only the FCC primitive cell and requiring the non-primitive cell to be rectangular.

2.2. Rectangular non-primitive cells for FCC primitive cells

Non-primitive cells with orthogonal axes have two distinct advantages over those with non-orthogonal axes: simplicity of programming and automatic specification of allowed small-cell wavevectors. The first point is immediately obvious; the second follows from vector analysis. If the three non-primitive cell direct lattice vectors are mutually orthogonal, then the general relation $\mathbf{A}_i \cdot \mathbf{B}_j = 2\pi\delta_{i,j}$ implies that $\mathbf{A}_i \| \mathbf{B}_i$, and hence the three non-primitive cell reciprocal lattice vectors are mutually orthogonal as well. Therefore, the non-primitive cell reciprocal lattice vectors lie along the axes of the non-primitive cell, and from Eq. (11) it is clear that some of the allowed small-cell wavevectors will lie along these directions. As shown in subSection 3.3 below, the shape of a particular non-primitive cell affects the sampling of allowed wavevectors, when a supercell composed of non-primitive rectangular cells is employed.

What is needed, then, is a practical method for choosing rectangular non-primitive cell, with one axis along a desired direction for a given crystal lattice. Because a completely general method tends to be difficult to implement, we instead make a few simplifying assumptions which lead to significantly clearer analysis and programming. In addition, we specialize our results to the FCC lattice, but the methods we use can be employed for other bulk lattices or even periodic nanostructures, such as superlattices [6] or nanowires [3] as well. The FCC primitive cell direct and reciprocal lattice vectors are

$$\mathbf{a}_1 = \frac{a}{2}(\mathbf{e}_y + \mathbf{e}_z), \quad \mathbf{a}_2 = \frac{a}{2}(\mathbf{e}_x + \mathbf{e}_z), \quad \mathbf{a}_3 = \frac{a}{2}(\mathbf{e}_x + \mathbf{e}_y) \tag{13}$$

$$\mathbf{b}_1 = \frac{2\pi}{a}(-\mathbf{e}_x + \mathbf{e}_y + \mathbf{e}_z), \quad \mathbf{b}_2 = \frac{2\pi}{a}(\mathbf{e}_x - \mathbf{e}_y + \mathbf{e}_z), \quad \mathbf{b}_3 = \frac{2\pi}{a}(\mathbf{e}_x + \mathbf{e}_y - \mathbf{e}_z) \tag{14}$$

where a is the FCC conventional unit cell cube edge. Without the loss of generality, we may take the non-primitive cell direct lattice vector $\mathbf{A}_1$ to lie along a specified direction. Its decomposition in terms of the Cartesian unit vectors is found using Eqs. (1) and (13)

$$\mathbf{A}_1 = \frac{a}{2}[n_1\mathbf{e}_x + n_2\mathbf{e}_y + n_3\mathbf{e}_z], \tag{15}$$

$$n_1 = m_{1,2} + m_{1,3}, \quad n_2 = m_{1,1} + m_{1,3}, \quad n_3 = n_1 + n_2 - 2m_{1,3}. \tag{16}$$

A few observations regarding Eqs. (15) and (16) are in order before proceeding. First, the form adopted by $\mathbf{A}_1$ must likewise apply to $\mathbf{A}_2$ and $\mathbf{A}_3$ as well. Second, n_3 is of the same parity as (n_1+n_2). From this, it follows that if n_1 and n_2 are of the same (opposite) parity then n_3 is even (odd). (We employ the term "parity" in the broadest sense, thus both +1 and −1 are said to be odd, etc). Thus, at least *one* of the coefficients n_i is even, and we choose n_3 even because this choice simplifies the analysis. Finally, not all directions are compatible as written with the form of Eqs. (15) and (16). For example, the shortest compatible axis along [111] is given by the trio $(n_1,n_2,n_3) = (2,2,2)$.

The analysis is further simplified by taking $\mathbf{A}_2$ to lie in the x–y plane. A choice which satisfies this criterion, along with $\mathbf{A}_1 \cdot \mathbf{A}_2 = 0$ is

$$\mathbf{A}_2 = \frac{a}{2}[-n_2\mathbf{e}_x + n_1\mathbf{e}_y] \tag{17}$$

with the obvious additional restriction that at least one of the integers n_1, n_2 be nonzero. Because $\mathbf{A}_2$ must satisfy the same form as $\mathbf{A}_1$, it follows from Eqs. (1) and (15) that

$$2m_{2,3} = n_1 - n_2. \tag{18}$$

Note that this equation is always satisfied under our simplifying assumption that n_1 and n_2 are of the same parity.

For the final supercell direct lattice vector, $\mathbf{A}_3$, a rectangular supercell requires that $\mathbf{A}_1 \cdot \mathbf{A}_3 = \mathbf{A}_2 \cdot \mathbf{A}_3 = 0$, and for convenience the sign of $\mathbf{A}_3$ is chosen to satisfy $(\mathbf{A}_1 \times \mathbf{A}_2) \| \mathbf{A}_3$. Using the form

$$\mathbf{A}_3 = \frac{a}{2}[pn_1\mathbf{e}_x + pn_2\mathbf{e}_y + (pn_1 + pn_2 - 2q)\mathbf{e}_z], \quad p, q \in \mathbb{Z} \tag{19}$$

we find

$$p = -(n_1 + n_2 - 2m_{1,3}), \quad q = -[n_1^2 + n_2^2 + n_1n_2 - m_{1,3}(n_1 + n_2)]. \tag{20}$$

If p and q have a greatest common divisor (GCD), a minimal-size supercell results by dividing both by their GCD. Substituting Eq. (20) into Eq. (19) results in an expression for $\mathbf{A}_3$ in terms of the original parameters

$$\mathbf{A}_3 = \frac{a}{2}[-n_1(n_1 + n_2 - 2m_{1,3})\mathbf{e}_x - n_2(n_1 + n_2 - 2m_{1,3})\mathbf{e}_y + (n_1^2 + n_2^2)\mathbf{e}_z], \tag{21}$$

where as desired, $\mathbf{A}_1 \times \mathbf{A}_2 = (a/2)\mathbf{A}_3$. Note that if n_1, n_2, and $m_{1,3}$ are such that $p = 0$, q becomes free and the shortest $\mathbf{A}_3$ comes from Eq. (19) directly, $q = \pm 1$, as discussed in Section 3.2 below.

Finally, it is useful to have expressions for the other $m_{i,j}$ in terms of n_1, n_2, and $m_{1,3}$

$$m_{1,1} = n_2 - m_{1,3}, \quad m_{1,2} = n_1 - m_{1,3} \tag{22}$$

$$m_{2,1} = -m_{2,2} = (n_1 + n_2)/2, \quad m_{2,3} = (n_1 - n_2)/2 \tag{23}$$

$$m_{3,1} = n_1^2 + m_{1,3}(n_2 - n_1), \quad m_{3,2} = n_2^2 + m_{1,3}(n_1 - n_2), \quad m_{3,3} = -n_1^2 - n_2^2 - n_1n_2 + 2m_{1,3}(n_1 + n_2). \tag{24}$$

Therefore, under our simplifying assumptions all of the remaining $m_{i,j}$ are specified by the three parameters n_1, n_2, and $m_{1,3}$.

2.3. Supercells of non-primitive cells

As discussed above, non-primitive rectangular cells are especially useful because some of the allowed small-cell wavevectors will lie along the non-primitive cell axes. These non-primitive cells may themselves be used as the unit cells for supercell calculations in order to achieve extra dense k-space sampling along a desired direction. This application is different from that of Fourier integration [7,8], where all the three supercell axes are the *same* multiple of the corresponding unit cell axes (i.e., $n\mathbf{A}_1$, $n\mathbf{A}_2$, and $n\mathbf{A}_3$). In general, a supercell composed of N_i non-primitive cells along the non-primitive cell axis $\mathbf{A}_i$ has supercell allowed wavevectors

$$\mathbf{K}_\mathbf{n} = \sum_{j=1}^{3} \frac{n_j}{N_j}\mathbf{B}_j, \quad \mathbf{n} = (n_1, \quad n_2, \quad n_3) \tag{25}$$

$$n_j = \begin{cases} -\dfrac{(N_j-2)}{2}, \ldots, -1, 0, 1, \ldots, \dfrac{N_j}{2}; & N_j \text{ even} \\ -\dfrac{(N_j-1)}{2}, \ldots, -1, 0, 1, \ldots, \dfrac{(N_j-1)}{2}; & N_j \text{ odd} \end{cases}. \tag{26}$$

There are thus $N_1N_2N_3$ supercell wavevectors given by Eq. (25). However, each (non-primitive) unit cell of the supercell has $M = |\det(\mathbf{M})|$ primitive cells, so that there are $MN_1N_2N_3$ small-cell wavevectors (shifted back into their first Brillouin zone if necessary)

$$\mathbf{k}_{\mathbf{n},i} = \mathbf{K}_\mathbf{n} + \mathbf{q}_i, \quad i = 0, 1, \ldots, M-1. \tag{27}$$

Observe that permitting different numbers of non-primitive cells along the three non-primitive cell axes allows one to more heavily sample $\mathbf{k}$ along one or more axes. For rectangular non-primitive cells, the density is further increased since often some of the $\mathbf{q}_i$ will lie along the desired axes.

3. Results

3.1. 2-FCC cell

This non-primitive cell has axes along [1 1 0], [$\bar{1}$ 1 0], and [0 0 1], and is well-suited for calculations of the small-cell bands along [1 1 0]. Using the development in Section 2 above, we take

$$n_1 = n_2 = m_{1,3} = 1 \tag{28}$$

so that the non-primitive cell direct lattice vectors are

$$\mathbf{A}_1 = \frac{a}{2}(\mathbf{e}_x + \mathbf{e}_y), \quad \mathbf{A}_2 = \frac{a}{2}(-\mathbf{e}_x + \mathbf{e}_y), \quad \mathbf{A}_3 = a\mathbf{e}_z \tag{29}$$

and $|\det(\underline{\mathbf{M}})| = 2$. Taking the origin of the cell to be at the upper right, front corner, the two primitive cells lie at

$$\boldsymbol{\rho}_0 = \mathbf{0}, \quad \boldsymbol{\rho}_1 = -\frac{a}{2}(\mathbf{e}_y + \mathbf{e}_z). \tag{30}$$

The non-primitive cell reciprocal lattice vectors are therefore

$$\mathbf{B}_1 = \mathbf{b}_3 + \frac{1}{2}(\mathbf{b}_1 + \mathbf{b}_2), \quad \mathbf{B}_2 = \frac{1}{2}(\mathbf{b}_1 - \mathbf{b}_2), \quad \mathbf{B}_3 = \frac{1}{2}(\mathbf{b}_1 + \mathbf{b}_2). \tag{31}$$

Note that any two of the $\mathbf{B}_i$ are related by a primitive cell reciprocal lattice vector, so only one is allowed as a small-cell wavevector, and

$$\mathbf{q}_0 = \mathbf{0}, \quad \mathbf{q}_1 = \mathbf{B}_3 = \frac{1}{2}(\mathbf{b}_1 + \mathbf{b}_2) = \frac{2\pi}{a}\mathbf{e}_z \tag{32}$$

$\mathbf{B}_3$ is chosen since it lies in the primitive cell first Brillouin zone.

3.2. 4 FCC cell

This case is the familiar FCC conventional unit cube studied at length in Refs. [2,5] and is the optimal rectangular cell for obtaining dispersions in the [1 0 0], [0 1 0], [0 0 1] directions. This cube is specified by the parameters

$$n_1 = 2, \quad n_2 = 0, \quad m_{1,3} = 1 \tag{33}$$

so that the non-primitive cell direct lattice vectors are

$$\mathbf{A}_1 = a\mathbf{e}_x, \quad \mathbf{A}_2 = a\mathbf{e}_y, \quad \mathbf{A}_3 = a\mathbf{e}_z \tag{34}$$

and $|\det(\underline{\mathbf{M}})| = 4$. Because $p = 0$, Eq. (19) was used to find the expression for $\mathbf{A}_3$ in Eq. (34) instead of Eq. (21). As noted above, this is the case in which q is free, and taking $q = -1$ in Eq. (19) results in a smaller non-primitive rectangular cell.

Once again choosing the origin of the rectangular cell to be the upper right, front corner, the four primitive cells are located at

$$\boldsymbol{\rho}_0 = \mathbf{0}, \quad \boldsymbol{\rho}_1 = -\frac{a}{2}(\mathbf{e}_x + \mathbf{e}_y), \quad \boldsymbol{\rho}_2 = -\frac{a}{2}(\mathbf{e}_y + \mathbf{e}_z),$$
$$\boldsymbol{\rho}_3 = -\frac{a}{2}(\mathbf{e}_x + \mathbf{e}_z) \tag{35}$$

The non-primitive cell reciprocal lattice vectors are all allowed as small-cell wavevectors, since none of them differs from another by a primitive-cell reciprocal lattice vector. Together with the zero vector (always allowed) they constitute the four allowed small-cell wavevectors

$$\mathbf{q}_0 = \mathbf{0}, \quad \mathbf{q}_1 = \mathbf{B}_1 = \frac{1}{2}(\mathbf{b}_2 + \mathbf{b}_3), \quad \mathbf{q}_2 = \mathbf{B}_2 = \frac{1}{2}(\mathbf{b}_1 + \mathbf{b}_3),$$
$$\mathbf{q}_3 = \mathbf{B}_3 = \frac{1}{2}(\mathbf{b}_1 + \mathbf{b}_2). \tag{36}$$

Because we have found $|\det(\underline{\mathbf{M}})|$ allowed small-cell wavevectors within the primitive-cell Brillouin zone, it follows that there are no other allowed small-cell wavevectors. For example, $-\mathbf{B}_1 = \mathbf{B}_1 - \mathbf{b}_2 - \mathbf{b}_3$ and so is not allowed.

3.3. 6 FCC cell

This non-primitive cell has axes aligned along directions [1 1 $\bar{2}$], [$\bar{1}$ 1 0], [1 1 1] and is useful for obtaining dispersions along the [1 1 1] direction. Note that from the discussion in Section 2.2 above the coefficients for the [1 1 1] axis will all be multiplied by 2 when Eqs. (15), (17), and (21) are used since that is the minimal such axis compatible with the FCC primitive cell direct lattice vectors. (The other two axes are compatible as written). Taking the [1 1 $\bar{2}$] axis to be $\mathbf{A}_1$ gives

$$n_1 = n_2 = 1, \quad m_{1,3} = 2. \tag{37}$$

The non-primitive cell direct lattice vectors are therefore

$$\mathbf{A}_1 = \frac{a}{2}(\mathbf{e}_x + \mathbf{e}_y - 2\mathbf{e}_z), \quad \mathbf{A}_2 = \frac{a}{2}(-\mathbf{e}_x + \mathbf{e}_y),$$
$$\mathbf{A}_3 = \frac{a}{2}(2\mathbf{e}_x + 2\mathbf{e}_y + 2\mathbf{e}_z), \tag{38}$$

with $|\det(\underline{\mathbf{M}})| = 6$. The slightly clumsy rendering of the expression for $\mathbf{A}_3$ is deliberate, in order to emphasize the factor of 2 which automatically results on application of Eq. (21). Rather than list the locations of the primitive cells within the non-primitive cell, we move to the more interesting case of the allowed small-cell wavevectors.

Eq. (5) gives the expressions for the non-primitive cell reciprocal lattice vectors. Here, it is more useful to represent them in terms of the primitive cell reciprocal lattice vectors:

$$\mathbf{B}_1 = -\frac{1}{6}\mathbf{b}_1 - \frac{1}{6}\mathbf{b}_2 + \frac{1}{3}\mathbf{b}_3, \quad \mathbf{B}_2 = \frac{1}{2}(\mathbf{b}_1 - \mathbf{b}_2),$$
$$\mathbf{B}_3 = \frac{1}{3}(\mathbf{b}_1 + \mathbf{b}_2 + \mathbf{b}_3). \tag{39}$$

Note that although $\mathbf{B}_2$ falls outside the primitive cell first Brillouin zone, $\mathbf{B}_2$+$\mathbf{b}_2$ lies within it (just on the surface, in fact). In addition, observe that because the coefficients of $\mathbf{B}_1$ and $\mathbf{B}_3$ are less than $\frac{1}{2}$ in magnitude, the four vectors $\pm\mathbf{B}_1$, $\pm\mathbf{B}_3$ are all allowed as small-cell wavevectors. On the other hand, because each has at least one coefficient of magnitude $\frac{1}{3}$, multiplying either by ± 2 would give a vector outside the primitive cell first Brillouin zone. With the zero vector and $\mathbf{B}_2$+$\mathbf{b}_2$, we have thus found the six allowed wavevectors for this non-primitive rectangular cell:

$$\mathbf{q}_0 = \mathbf{0}, \quad \mathbf{q}_1 = \mathbf{B}_1, \quad \mathbf{q}_2 = \mathbf{B}_2 + \mathbf{b}_2, \quad \mathbf{q}_3 = \mathbf{B}_3, \quad \mathbf{q}_4 = -\mathbf{B}_1,$$
$$\mathbf{q}_5 = -\mathbf{B}_3. \tag{40}$$

Again, we emphasize that because the primitive-cell Brillouin zone is $|\det(\underline{\mathbf{M}})| = 6$ times larger than that of the non-primitive cell, there are only six allowed small-cell wavevectors. Thus once six have been found within the primitive-cell first Brillouin zone, we are guaranteed that they are the only ones.

3.4. Zone unfolding with the 6 FCC cell

As an example use of these cells, we compare the bands of Ge as calculated with the single-primitive unit cell and as unfolded from a supercell composed of non-primitive 6 FCC cells (subSection 3.3 above). This type of calculation is a necessary test for any supercell electronic structure code because the supercell results must agree with the single primitive cell results, when all primitive cells are identical. In both cases, the $sp^3d^5s^*$ spin-orbit tight-binding model [13] is used, with Ge parameters from Ref. [14]. The supercell is based on the non-primitive 6 FCC cell, with 20 of these cells along its [1 1 1] axis and 2 cells along each of the other orthogonal axes in order to achieve good resolution of the Ge conduction band. Fig. 1 shows the bands of Ge from Γ to L as calculated directly from the single-primitive cell $sp^3d^5s^*$ spin-orbit Hamiltonian (solid lines) and as unfolded [2,4,6] from the $20 \times 2 \times 2$ supercell (diamonds). As expected, there is excellent

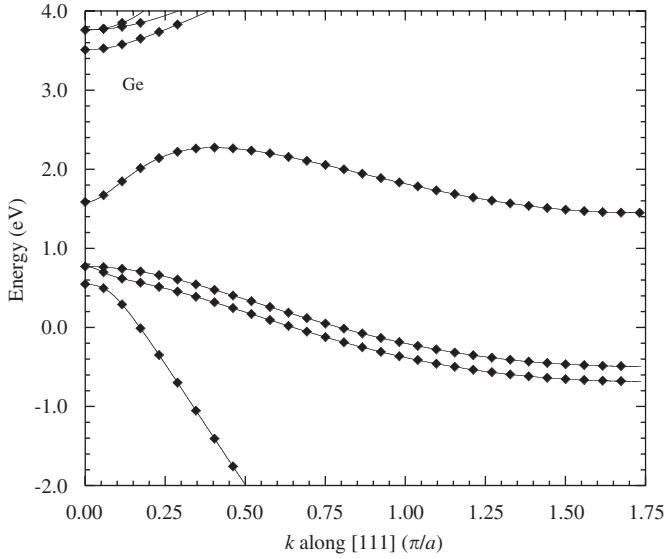

Fig. 1. Bands of Ge from Γ to L as calculated directly from the single-primitive cell $sp^3d^5s^*$ spin-orbit Hamiltonian (solid lines) and as unfolded from the $20\times2\times2$ supercell (diamonds). The supercell is based on the non-primitive 6 FCC cell and has 20 cells along [1 1 1] and 2 cells along each of the other axes. Note the excellent agreement between the two methods.

agreement between the two methods. We note here that we have previously used the non-primitive 4 FCC cell in AlGaAs approximate bandstructure calculations [2].

4. Conclusions

We have developed a simple, easily implemented method for determining the allowed wavevectors in non-primitive rectangular cells for the FCC lattice. This method is especially useful, because non-primitive rectangular cells for the FCC lattice can have at most one axis aligned with a primitive cell axis, so that the simple case treated in solid state texts is no longer applicable. We have also presented general relations for allowed wavevectors in any non-primitive cell, irrespective of the underlying primitive cell. For rectangular non-primitive cells, the shortest non-primitive cell reciprocal lattice vectors are parallel to the non-primitive cell real-space axes, so that the allowed wavevectors for the non-primitive cell will lie in these directions as well. Finally, we have illustrated the use of non-primitive rectangular cells in tight-binding supercell calculations by unfolding the bands of Ge from a supercell based on the 6 FCC cell presented here.

Acknowledgments

This work was supported by Semiconductor Research Corporation. The work described in this publication was carried out in part at the Jet Propulsion Laboratory, California Institute of Technology under a contract with the National Aeronautics and Space Administration, and Jet Propulsion Laboratory. nanohub.org computational resources provided by the Network for Computational Nanotechnology, funded by the National Science Foundation were used.

References

[1] G. Klimeck, F. Oyafuso, T.B. Boykin, R.C. Bowen, P. von Allmen, Comput. Modeling Eng. Sci. 3 (2002) 601.
[2] T.B. Boykin, N. Kharche, G. Klimeck, M. Korkusinski, J. Phys.: Condens. Matter 19 (2007) 036203.
[3] T.B. Boykin, M. Luisier, A. Schenk, N. Kharche, G. Klimeck, IEEE Trans. Nanotechnol. 6 (2007) 43.
[4] T.B. Boykin, G. Klimeck, Phys. Rev. B 71 (2005) 115215.
[5] T.B. Boykin, N. Kharche, G. Klimeck, Eur. J. Phys. 27 (2006) 5.
[6] T.B. Boykin, N. Kharche, G. Klimeck, Phys. Rev. B 76 (2007) 035310.
[7] S. Froyen, Phys. Rev. B 39 (1989) 3168.
[8] R. Ramirez, M.C. Bohm, Int. J. Quantum Chem. 34 (1988) 578.
[9] N.W. Ashcroft, N.D. Mermin, Solid State Phys., Saunders College, Philadelphia, 1976 (Chapters 5, 8).
[10] W.A. Harrison, Solid State Theory, Dover, New York, 1979 (Section 2.1).
[11] C. Kittel, Introduction to Solid State Physics, Wiley, New York, 1996 (Chapter 7).
[12] J.M. Ziman, Principles of the Theory of Solids, second ed., Cambridge University Press, New York, 1972 (Section 1.6).
[13] J.-M. Jancu, R. Scholz, F. Beltram, F. Bassani, Phys. Rev. B 57 (1998) 6493.
[14] T.B. Boykin, G. Klimeck, F. Oyafuso, Phys. Rev. B 69 (2004) 115201.